ISSN 0511-5728
The West Indian Journal of Engineering
Vol.38, No.1, July 2015, pp.41-51

Flame Detection and Suppression System for Petroleum Facilities

Olawale S. Ismail [a,Ψ] and Chimsom I. Chukwuemeka[b]

Department of Mechanical Engineering, Faculty of Technology, University of Ibadan, Ibadan, Nigeria
[a]E-mail: os.ismail@ui.edu.ng
[b]E-mail: chukwuemeka.ci@gmail.com

[Ψ] *Corresponding Author*

(Received 04 November 2014; Revised 02 July 2015; Accepted 30 July 2015)

Abstract: *An adaptive model for fire (flickering flame in the infrared region) detection and subsequent suppression is presented. The model applies a Pyro-electric Infrared sensor (PIR)/Passive Infrared Detector (PID) for infrared fire detection. Sample analog signals were generated and simulated within the framework of the modeled PIR sensor/PID. The signals were modeled around the flame flicker region (1-13Hz) and outside the region. A Joint Time Frequency Analysis (JTFA) function was applied to model the Digital Signal Processing (DSP). This involved extraction of fire and non-fire features from the sample signals. A Piecewise Modified Artificial Neural Network (PMANN) and the Intraclass Correlation Coefficient (ICC) were employed in the decision framework. The PMANN generated polynomials which analysed and 'memorised' the signals from DSP. The ICC further categorised cases as 'fire' or 'non-fire' by comparing data from the PMANN analyses. In cases of detected fire, valves to several fire suppression systems (like water sprinklers and foam injection lines) can be opened. Hence, the Solenoid Hydraulic Valve was modelled to be controlled by a Proportional Integral Derivative Controller (PIDC). The whole model of detection and suppression can be further developed, studied and subsequently implemented.*

Keywords: *Flame detection, passive infrared detector, digital signal processing, artificial neural networks, fire suppression*

1. Introduction

Petroleum facilities, also known as oil and gas storage facilities are sites where combustible/flammable liquids are received from shipping vessels, pipelines, tankers etc. These products can be stored or blended in bulk for the purpose of distribution by tankers, pipelines and other methods of transfer and transportation. From this definition, one expects the observation of very high safety standards on such sites to prevent loss of any kind especially by fire. Despite the progress made in the design and installation of safety facilities for oil storage sites, they remain one of the most hazardous places on earth. Late detection and/or suppression of fires are among the primary reasons why little fire outbreaks leads to major oil storage site fire disasters. Two studies on petroleum facilities (Persson and Lonnermark, 2004 and James and Cheng-Chung, 2006) listed the following as the main causes of fire outbreaks in oil and gas storage sites: lightning, maintenance error, operational error, sabotage, equipment failure, crack and rupture, static electricity, leak and line rupture, open flames, natural disasters and runaway reactions. The results show that most fires in these storage sites primarily affect the tanks, with lightening being the main cause of fire outbreaks.

Even though many problems can be traced to fire outbreaks in oil storage sites, usually their spread is associated with low quality engineering. A model solution is proposed to the problem of early detection and automatic suppression. This particular problem is most rampant in oil and gas storage sites in local Nigeria as well in some other developing nations. Although several enhanced fire prevention/fighting engineering mechanisms are already being employed to mitigate this problem, research and development of new and better ones still continue. This work is just another window into that wide field of research.

2. Related Work

The use of fire detection systems incorporated with fire suppression started with Philip W. Pratt of Abington, in 1872 ("Automatic fire suppression," 2015, para 2). He patented the first automatic sprinkler system. Thus, there was a detection system in his design that automatically actuated the sprinklers. Generally, from the anatomy of fire, represented by Equation (1). There are four (4) main areas of fire detection: smoke, gas (like CO_2, CO, H_2S, etc.), heat and light. The light emitted cover both the infrared and ultraviolet regions.

$$\mathrm{HC(hydrocarbon)} + \mathrm{O2(g)} + \mathrm{Energy}_{(\mathrm{absorbed})} \rightarrow \mathrm{CO2(g)} + \mathrm{H2O(vap)} + \mathrm{Heat}_{(\mathrm{released})} + \mathrm{light} + \mathrm{other\ gases} \quad (1)$$

Conventional smoke detectors typically detect the presence of certain particles generated by smoke and (1) by ionization or photometry. An important weakness of such detectors is that the smoke has to reach the sensor. For heat detectors, the heat must be sufficient enough to activate the heat sensor. This may take a significant amount of time to issue an alarm. The time delay can cause an uncontrollable fire to develop. Therefore, it is not possible to use them in open spaces. For UV detectors, they are plagued by many false alarm signals, which reduce their reliability (Nolan, 1996). With minimal and controllable false alarms (using sophisticated detection algorithms), infrared detection remains the most reliable.

Several detection algorithms have been applied over time in the area of infrared flame detection. Some of the prominent algorithms include the statistical analysis of the apparent source of the heat of fires (Zhu et al, 2008) at a near infrared zone. After tests and experimentations, it was concluded that the detector functioned well for open flames, producing very few false alarms, while smoldering fires were hardly detected, since there was no direct radiation to the detector. They were only detected when they had direct radiation. Several Advanced Very High Resolution Radiometer (AVHRR) fire detection algorithms were reviewed in another study (Li et al 2000). The study aimed at uncovering their principles of operation and limitations, while also making possible recommendations for improvement.

Moreover, an adaptive method for hydrocarbon flame detection was developed using a Joint Time Frequency Analysis (JTFA) functions for Digital Signal Processing (DSP) and Artificial Neural Network for the decision mechanism (Javid et al., 2008). The JTFA functions used were the Short Time Fourier Transform (STFT) and The Fast Fourier Transform (FFT), with the Hamming Window function applied to narrow the coefficients to a particular range. That study gave convincing results and was eventually developed into a marketable practical application. Furthermore, using the Markov Model decision algorithm and Lagrange wavelet filter banks to extract fire features from signals recorded by pyro-electric infrared sensors, a fire detector was modeled which could easily detect fire within the flickering flame frequency (Fatih et al., 2012). Out of 220 fire test sequences, they recorded 3 false alarms and 217 correct alarms. Each detection had a response time of 77seconds.

Some of the most prominent suppression systems include fire water distribution systems, sprinkler systems, water spray and deluge systems, water flooding systems, fire water control and isolation valves (Nolan, 1996). In developing countries (e.g. Nigeria), the pipelines supplying water or other fire suppression liquids to these systems contain manually operated valves. This slows down the process of suppression during emergencies. However, by applying automatically actuated valves as proposed in this work, it will ease the fire suppression process. Proportional Integral Derivative Controllers (PIDC) has been applied in many areas to automatically actuate valves. Some of the applications include the study of The Position Control System of a hydraulic cylinder based on microcontrollers (Munaf, 2008). Using the MATLAB software, a PIDC in connection to the hydraulic valve was simulated. The purpose was to use the controlling mechanism of the PIDC to cause the cylinder to function automatically. Besides, pneumatic actuator systems were designed and controlled using PIDCs and valves (Lai et al., 2012). The pneumatic systems, being non-linear, were controlled using linear control mechanisms like PID controllers and valves.

This work used an algorithm which applied the Discrete Wavelet Transform (DWT) (a JTFA function) for DSP, a Piecewise Modified ANN (PMANN) and the Intraclass Correlation Coefficient (ICC) for the decision framework. The DWT made on-line analysis and feature extraction of signals possible with the shortest time delay. The PMANN analysed and ‘memorised’ data (from the DSP) that could be easily matched for “fire” and “non-fire” cases using the ICCs. It further applied the PIDC to control a solenoid hydraulic valve, which is commonly used in petroleum facilities. Figure 1 shows the flow chart for the model adapted in this work.

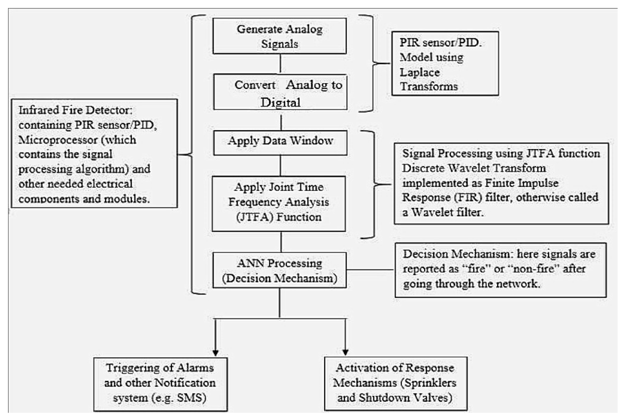

Figure 1. Flow Chart for the modeling of Fire Detection and Suppression System

3. Methodology

3.1 The Pyro-Electric Infrared Sensor (PIR)/Passive Infrared Detector (PID)

A PIR sensor/PID is comprised of three main parts, namely the Fresnel lens (which focuses the IR radiation to the sensor), the PIR sensor which senses the IR radiation and an amplifier/comparator or amplifier/ analog to digital converter (ADC) circuitry depending on the generation of the PID (Emin, 2009). The Fresnel lens offers a field of view (FOV) of 110o over a distance of 11m. This work simulated the third generation PID, where the comparator circuitry is replaced by analog to digital converter (ADC) as shown in Figure 2. Hence, after amplification, we have the ADC. The ADC gains were then fed into a microprocessor containing the detection algorithm for further signal processing and categorisation decision (if the model is to be implemented).

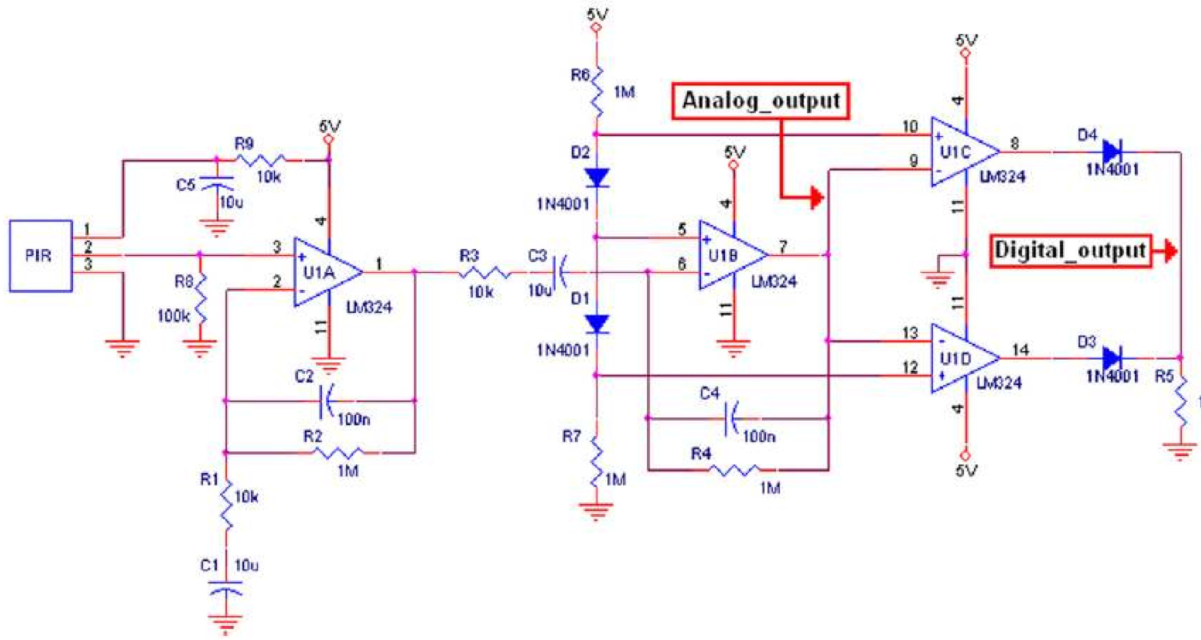

Figure 2. Third Generation PID circuitry for capturing analog signals and converting them to digital signals

Such a sensor/detector can be modeled as a capacitor with capacitance Cd with a Poly-Vinylidene Fluoride **(**PVDF) film as the dielectric with thickness d and surface area A (Odon, 2010). When IR radiation of power Φ(t), varying in time is incident on the active surface of the PIR sensor, an electric charge q(t) is generated. This is transferred as a signal with information content either as voltage V(t) on the detector electrodes or current Ip(t) flowing through the low load resistance of the detector output. Converting IR radiation into an electric signal is done in 3 stages: converting radiation power Φ(t) to thermal change on the sensor surface i.e. temperature ΔT(t), the second stage is the thermal to electric conversion i.e. ΔT(t) to Ip(t), and the last stage is the current to voltage signal conversion i.e. Ip(t) to V(t). The PID detects infrared radiations from several sources within its range or field of view.

From automatic control theory, the procedures for the creation of block diagrams for simulation involves connecting the block transfer function in series, where series connection implies multiplication. For our model, we arranged them in the order: $G_T(s)$ (radiation to thermal), $G_{TIp}(s)$ (thermal to electrical) and $G_{IpV}(s)$ (electrical to voltage), describing properties of the appropriate signal conversion stage. Hence, the equivalent transfer function is expressed as Equation (2) and a schematic of the process is shown in Figure 3:

$$G(s) = G_T(s) \times G_{Tip}(s) \times G_{IpV}(s) \tag{2}$$

A Laplace transfer function was developed for the simulation, expressed as Equation (3) (Odon, 2010):

$$G(s) = \frac{p\eta R}{c'dC} \cdot \frac{s\tau_{th}\tau_e}{s(s\tau_{th}+1)(s\tau_e+1)} \tag{3}$$

where p is the pyro-electric coefficient, η-absorption coefficient of radiation, R-equivalent resistance, C-equivalent capacitance, d-thickness of PVDF film, c prime-volume specific heat, τ_{th} -thermal time constant and τ_e -electric time constant. Using values for a standard detector with small PVDF thickness, sample IR radiations around the flickering flame frequency (1-13Hz), and also far from it, were generated and simulated on the MATLAB/SIMULINK software as shown in Figure 4. The values for the various parameters were obtained from standard values for PVDF IR sensor (Piezo Film Sensors Technical Manual by Measurements Specialties Inc.) and from other test results (Odon, 2010). The values of parameters for the PVDF PIR sensor/PID are outlined in Table 1.

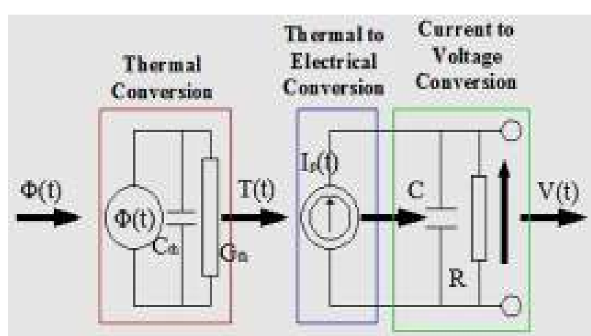

Figure 3. Schematic Diagram for Conversion of IR radiation to Voltage Signal

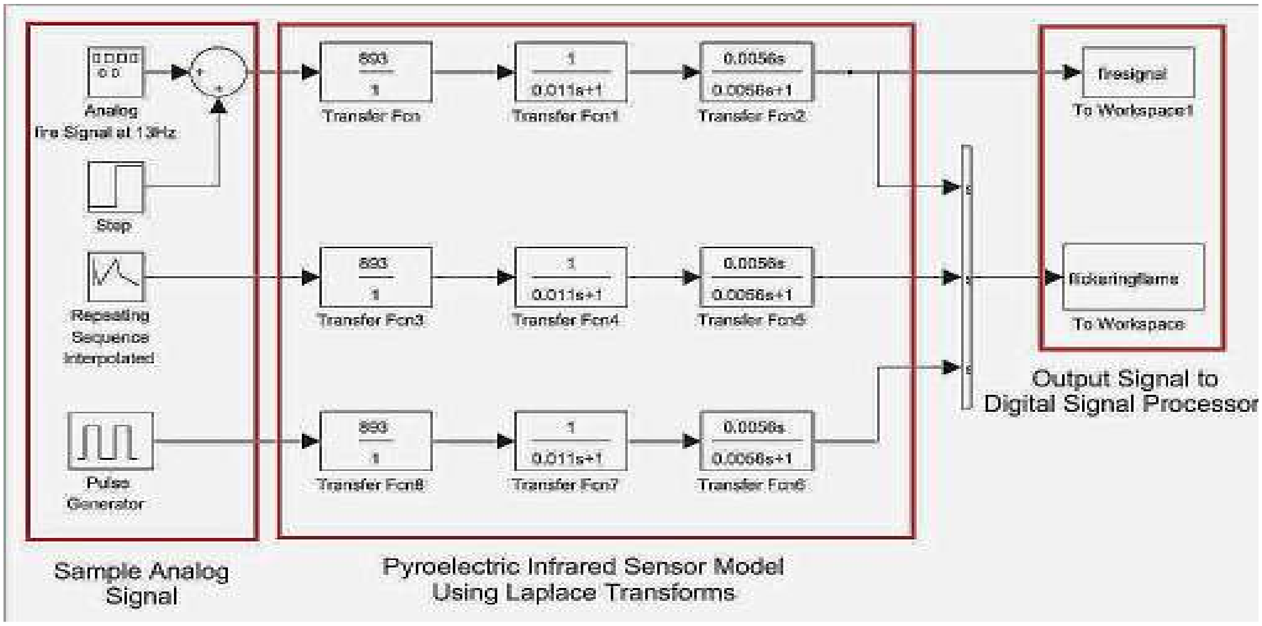

Figure 4. MATLAB/SIMULINK block for sample flickering flame signal (13Hz)

Table 1. Parameters for the PVDF PIR sensor/PID

Name	Value	Unit
Pyro-electric coefficient p	3×10^{-6}	C/cm^2.K
Volume specific heat c'	2.4	J/cm3.K
Permittivity ε	106×10^{-14}	F/cm
PIR film thickness d	25	Mm
Thermal conductivity gth	0.00135	W/cmK
Detector active surface A	132×10^{-2}	Cm^2
PIR detector Capacitance Cd	560	pF
Amplifier input capacitance CL	Negligible	pF
Amplifier input resistance RL	10	MΩ
Absorption coefficient of radiation η	1	-
Electrical time constant of detector-amplifier circuit τe	0.0056	S
Thermal time constant τth	0.0110	S

3.2 The Detection Algorithm

3.2.1 Digital Signal Processing

The digital signal processing algorithm was developed using the Discrete Wavelet Transform (DWT) JTFA function implemented in real-time as wavelet filters (Schneiders, 2001). The signals were first passed through a window function (the Hamming window) to attenuate the input signal, thereby reducing spectral leakage and causing the signal to be more periodic. A window length of 256 was chosen. This is advantageous since it reduces the response time of the detection mechanism by two (Javid et al., 2008). The window function is expressed as in Equation (4) (Robert, 2012),

$$w(n) = \frac{1}{2}\left\{1.08 - 0.92\cos\left(\frac{2\pi n}{N-1}\right)\right\} \quad (4)$$

With a 256 window length, a Nyquist sampling frequency of 50Hz was chosen. The flickering flame frequency of 13Hz (Fatih et al., 2012) was used as the cutoff frequency. The Nyquist sampling frequency is determined from $f_s \geq 2$ (cutoff frequency). Applying the formula, we get 26Hz as our sampling frequency. But a 50Hz sampling frequency was chosen to widen the frequency range in order to obtain a better sampled signal.

For real signals, only half of the number of samples (the same as the window length) contains essential information without redundancy. Hence, using Rayleigh's Limit (Robert, 2012), the frequency resolution is expressed as Equation (5), which becomes Equation (6) for the signals:

$$\Delta f = \frac{f_s}{N} \quad (5)$$

$$\Delta f = \frac{f_s}{0.5N} \Rightarrow \Delta f = \frac{50Hz}{(0.5)256} = 0.4Hz \quad (6)$$

Real-time wavelet filters are defined by their Quadrature Mirror Filters (QMF) used for DWT. QMFs are perfect reconstruction filter banks where the calculation of coefficients for the filters at all levels is seen as making an orthonormal (orthogonal and normalised) projection onto a new base. These filters banks contain highpass (H) and lowpass (L) filters of length N+1 (Schneiders, 2001), where N is the number of points or filter order which is the same as window length.

Depending on the number of levels, denoted as P, the analysis filter was applied to the input signal to calculate coefficients for the first level. Using N old input points, the coefficient was then calculated for the next level. Hence, the total number of old input samples needed for computation of a new coefficient at a certain decomposition level is defined by Equation (7) (Schneiders, 2001):

$$l_u = \sum_{i=1}^{P} N 2^{i-1} \tag{7}$$

where i is the decomposition level varying between 1 and the maximum, P, and N the order of the original filters. From this point, coefficients were obtained as the output at each level. This way made on-line analysis and feature extraction possible with the shortest time delay for each decomposition level. This is good for real time situations like flickering flames and other radiation emitting objects. Such structure was built on the MATLAB software. The code produced a filter matrix A, which was implemented as discrete (Finite Impulse Response) FIR filter block on MATLAB/SIMULINK. Since all coefficients are updated at every sample hit, the time resolution increased. Hence, for filter structure as a wavelet analyser the time resolution is expressed as Equation (8) (Schneiders, 2001):

$$\Delta t = \frac{1}{f_s} \tag{8}$$

The time-resolution is equal to the sample time of the system. For the DWT perfect reconstruction multi-resolution tree the frequency resolution is a function of the decomposition level P expressed as Equation (9) (Schneiders, 2001):

$$\Delta f = \frac{f_s}{2^{P+1}} \tag{9}$$

Using the values for sampling frequency and frequency resolution, the time resolution was determined and decomposition level was set to be Δt = 0.02s and P = 6 as shown below.

$$\Delta t = \frac{1}{f_s} = \frac{1}{50Hz} = 0.02s \tag{10}$$

And from Equation (6), we had

$$0.4Hz = \frac{50Hz}{2^{P+1}}, \text{where } P \approx 6.0\ . \tag{11}$$

Using N=256 points, the filter lengths were calculated as: L = H = N + 1 = 256 + 1 = 257

Substituting the values for the number of points N, filter lengths for the highpass (H) and lowpass (L) filters and the decomposition level P into our MATLAB code generated the needed coefficients. These coefficients were substituted into the Finite Impulse Response (FIR) filter block on MATLAB/SIMULINK software, as shown in Figure 5. Hence, the block was renamed 'Wavelet Filter'. The coefficients obtained are given in the matrix A.

A = {0.00, 2.82, 0.00, 0.00, 0.00, 0.00}

The digital signal processing as described here ensures that specific features of the signal are extracted, so that false alarms can be reduced to the barest minimum.

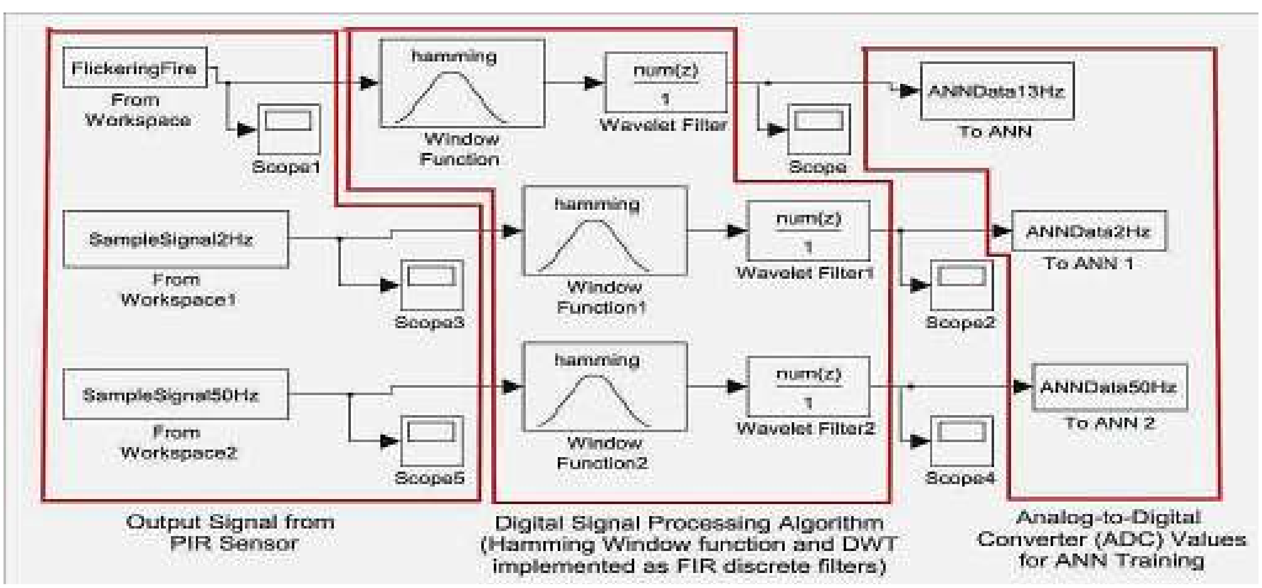

Figure. 5 MATLAB/SIMULINK block for sample flickering flame signal (13Hz)

3.2.2 The Decision Mechanism

An Artificial Neural Network (ANN) algorithm and the Intraclass Correlation Coefficient (ICC) constituted the decision rule. Previous research employed neurons and several complex scaling parameters to classify the network and get the desired output (Javid et al., 2008). The use of neurons for ANN is very difficult and complex. Hence, in this model neurons were not used. Instead the algorithm made use of polynomial approximations or the Least Squares approximation method, whereby polynomial equations were generated to establish a link between the input and the output (Chukwuka, 2014).

For this algorithm, the input parameters were distributed into the network, rather than lumping them into the network. Lumping the inputs into the network creates several errors while distributing them reduces these errors (Chukwuka, 2014). Four (4) distributions were made, which generated four equations resulting in a Piecewise Modified ANN (PMANN). Figures 6 and 7 are the algorithm flow charts.

The polynomial generated for our own case is expressed as Equation 12 (Chukwuka, 2014):

$$\text{"}Fire\text{" or "}Non-fire\text{"} = \sum_i^k (a_i + b_i x_i + c_i x_i^2 + d_i x_i^3) \quad (12)$$

where k is the number of inputs being considered. For the purpose of simulation k=3. But the network was trained with the model flame flicker frequency (13Hz) signal, so that it would be able to differentiate fire cases from non-fire during simulation.

Let Wi be the input weights and Sfi their scaling factor, and ai, bi, ci and di be the coefficients of each input considered. The coefficients are expressed as in Equation (13):

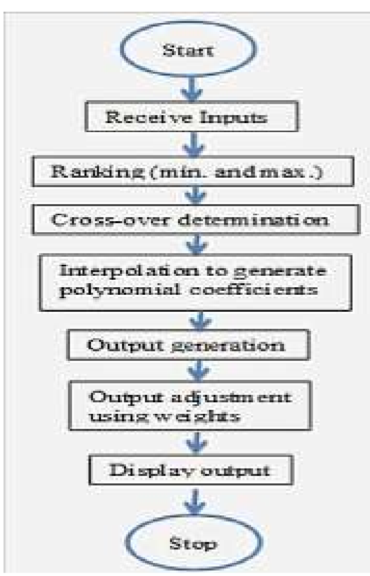

Figure 6. Flow Chart for proposed PMANN

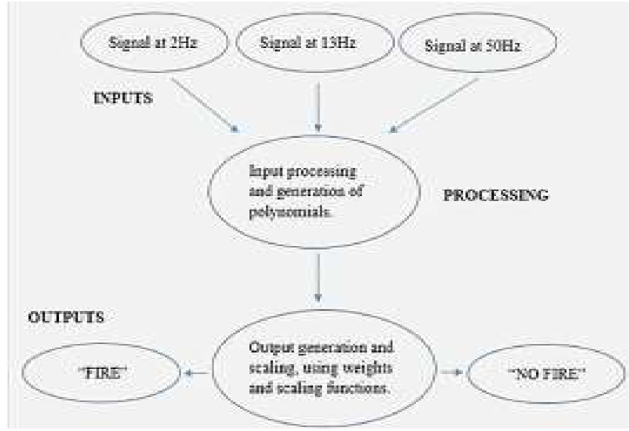

Figure 7. Inputs and Outputs of the Neural Network

$$a_i = a \times Sf_i \times W_i$$
$$b_i = b \times Sf_i \times W_i$$
$$c_i = c \times Sf_i \times W_i$$
$$d_i = d \times Sf_i \times W_i \quad (13)$$

For this model and simulation, the weight was set to be Wi = 1.0 and scaling factor to be Sfi = 0.01. This simplified the scaling process, making the equations easily evaluated within the framework of the network. The coefficients obtained could be matched for 'fire' and 'non-fire' cases using simple statistical correlations like the ICC. The algorithm was designed to receive inputs, sort them out, adjust their parameters and compute the expected result. The polynomial equations obtained from the above analysis were logged into a MATLAB m-file. The ensuing programme ran for different data sheets containing signal coefficients from the DSP.

Using the Intraclass Correlation Coefficient (ICC), data from the PMANN analysis are differentiated into "fire" and "non-fire" cases. The ICC is used to quantify the degree to which measurements with a fixed degree of relatedness match each other in terms of quantitative trait. Besides, this statistical analysis can be applied to assess the consistency (or agreement) of quantitative measurements made by different observers measuring the same quantity. All these are classified as reliability analysis. Hence, this method was applied to analyse the data gotten from PMANN. The coefficients obtained from the data of sample signals of frequency 2Hz, 50Hz and 13Hz (fire signal) were matched against those of the 13Hz (fire signal) used for training.

For a perfect match, the scenario was recorded as "fire" otherwise it was recorded as "non-fire". This analysis was carried out on the SPSS 16.0 software. The results obtained were for the "class 2" or "two-way" random single and average measures (consistency/ absolute agreement) ICC with a 95% confidence interval. Here, the measurement raters are chosen at random. The reliability of the analysis is interpreted between the lower and upper bound of the confidence interval (see Figure 8).

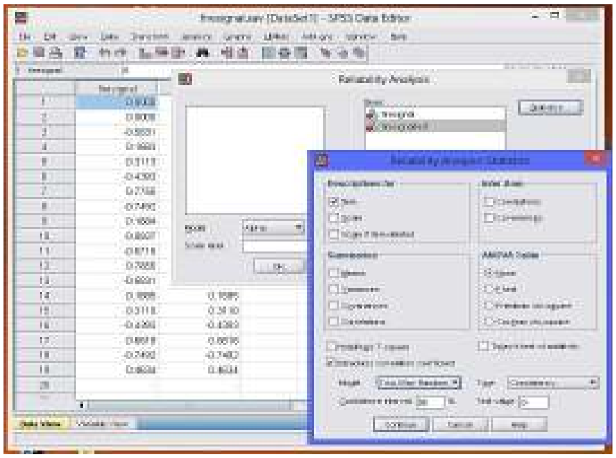

Figure 8. SPSS ICC Reliability Analysis

3.2.3 Suppression Mechanism

The fire suppression response mechanism involved the modeling of control valves. The aim was to come up with a model that could be able to control (open/close) fire suppression systems (foam injection lines, water deluge lines, and water sprinkler lines, etc.), pipelines and also active pumps. By using Proportional, Integral and Derivative Controllers (PIDCs), we simulated the control of an Active Hydraulic Device (ADH) such as hydraulic proportional valves (Yong, 2009).

Under normal system operations in these sites, pumps used for loading and unloading of petroleum products are always running to keep business moving. Also, fire pipelines for suppression systems are always pressurised for emergency cases. These valves can be connected at key places along these pipelines, such that immediately this model detector senses fire, signals are sent to these valves for prompt control as the case may demand.

Developed out of the ineffectiveness of the Proportional (P) and Proportional Derivative (PD) controllers, the PIDCs are better in function and response since they integrate the Proportional (P) and Proportional Derivative (PD) controllers. They have several applications, including use at oil and gas storage sites.The conve ntional PID equation is expressed as Equation (14) (Yong, 2009)

$$U(t) = K_c(e + \frac{1}{T_i}\int_0^t e dt + T_d \frac{de}{dt}) \tag{14}$$

where e is the controller error, that is the deviation of the process variable u(t) from its set point uo. Constants KC, Ti and Td are, respectively, the proportional gain, integral time and derivative time constants of the PIDC. They represent the characteristics of the controller. The Laplace transfer function is expressed as in Equation (15) (Katsuhiko, 2010).

$$\frac{U(s)}{E(S)} = K_c\left(1 + \frac{1}{T_i s} + T_d s\right) \tag{15}$$

In determining the values for Kc, Ti and Td for simulation, the Zeigler-Nichols method of tuning PIDCs was used (Katsuhiko, 2010). The method has two (2) approaches, the process reaction method and continuous cycling method. For the model, the process reaction method was applied.

This is based on the assumption that the open-loop step response of most process control systems has an S-shape, called the process reaction curve. It is characterised by two (2) constants, the delay time L and time constant T. For the PIDC K_c = 1.2T/L, T_i = 2L and T_d = 0.5L. Substituting these into Equation (16), the Laplace transfer function becomes

$$\frac{U(s)}{E(S)} = \frac{0.6T(s+1/L)^2}{s} \tag{16}$$

Generally, the control system makes the hydraulic device active. So, the head-discharge relationship of an AHD is usually dynamically modified via its control system to change the opening or closing of its control valve. The generalised dynamic characteristics of an AHD are expressed as Equation (17) (Yong, 2009):

$$F\left(Q, H, Y, \frac{dy}{dt}, \dots\right) = 0 \tag{17}$$

where Y corresponds to the solenoid of a hydraulic proportional valve. Electric signals from a PIDC are directed to the solenoid to either open/close the valve. Q is flow rate and H is the head.

The solenoid of the hydraulic valve was assumed to have first order dynamics (Roland, 2001) expressed by Equation 18:

$$\frac{V}{U}(s) = \frac{K_v}{1+T_i s} \tag{18}$$

Using standard manufacturer values for a PIDC (Munaf, 2008), the hydraulic proportional valve was simulated on MATLAB/SIMULINK interface as shown in Figure 9.

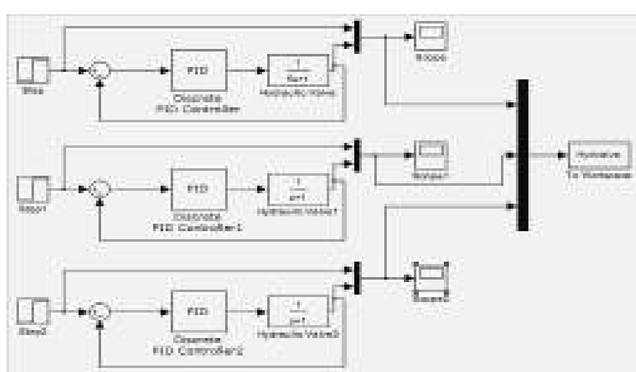

Figure 9. MATLAB SIMULINK block diagram for Hydraulic Valve Response

The values were varied to get different responses for the same hydraulic valve constant (Munaf, 2008):

Kc = [5, 5, 2], *Ti* = [5, 1, 1], Td = [2, 1, 2] and valve constant Kv = 1.0

Changing *Ti* from the valve dynamic equation also changed its response to the PIDC. Generally, signal flow through the whole model is as shown in Figure 10.

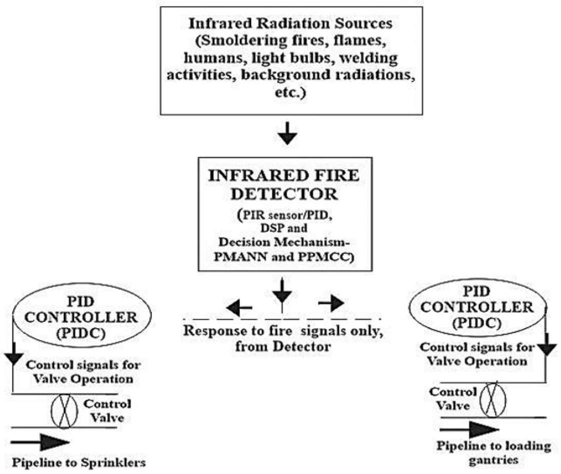

Figure 10. Signal Flow for whole model

4. Results and Discussion

Figures 11, 12 and 13 were obtained after infrared signals modeled at the flickering frequency (13Hz), and other frequencies for example 2Hz and 50Hz were simulated using the MATLAB/SIMULINK block for the PIR sensor/PID, respectively.

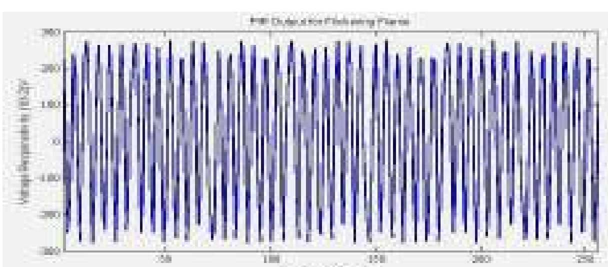

Figure 11. PIR Sensor/PID Output for fire at 13Hz

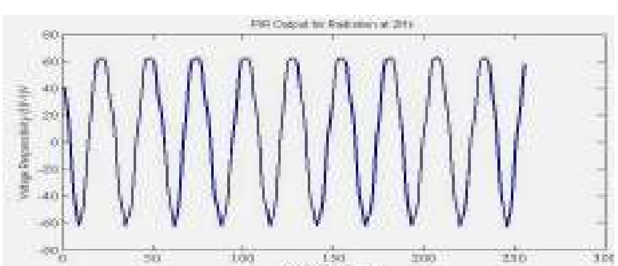

Figure 12. PIR Sensor/PID Output for radiation at 2Hz

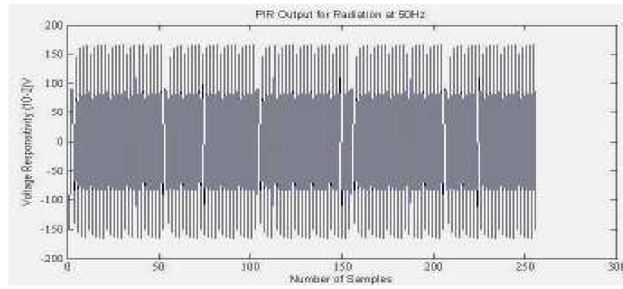

Figure 13. PIR Sensor/PID Output for radiation at 50Hz

From these figures, the difference among the various radiations can easily be seen. A step function, sequence interpolator and pulse generator (see Figure 4) were added together to generate the IR analog signals. This accounted for the oscillatory nature of the graphs. The fire radiation produced higher values (from -3 and 3 V) for voltage responsivity. If the model is to be implemented, the voltages are fed into a microcontroller with the Digital Signal Processing algorithm (DSP). A similar case was achieved when the voltages were fed into the MATLAB/SIMULINK interface containing the corresponding DSP blocks discussed earlier (Figure 4).

For a Hamming window length of N = 256 and wavelet filter implemented on SIMULINK as a discrete Finite Impulse Response (FIR) filter block, the 256 samples (or coefficients) considered by the window function were filtered and the recorded samples narrowed down to 52 samples (or coefficients). This further fine-tuned the detection process, for the results of the signal processing for a simulation time of 10 seconds. After DSP, each signal produced coefficients which were fed into the PMANN for the decision mechanism.

Out of the 52 samples (or coefficients) produced by the DSP algorithm, 18 were used in the training of the network (these contains recorded information i.e. non-zero samples as seen from Figures 14, 15 and 16). The other 34 samples (or coefficients) could be rounded up/down to zero; hence, they were not needed for the training. The DSP output from the model fire signal (13Hz) was our measured and expected output. Therefore, it was used to train our network. After training and classification, the other signals (2Hz and 50Hz) were then passed through the network for analysis. Below are the results for the training and analysis.

The blue graph is the expected (measured) output of PMANN, while green is graph for the signal under analysis (predicted). Figure 17 shows the training of the network, hence, perfect match between the predicted and measured. While Figures 18 and 19 are the results of the analysis.

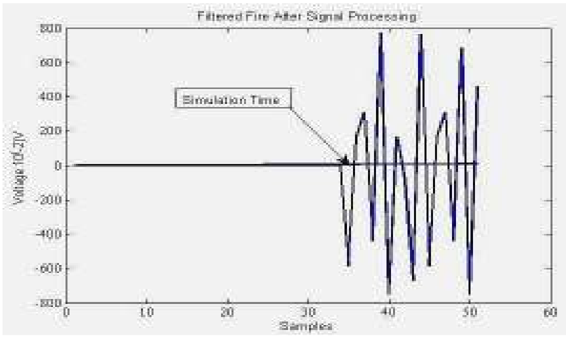

Figure 14. Radiation at 2Hz after DSP

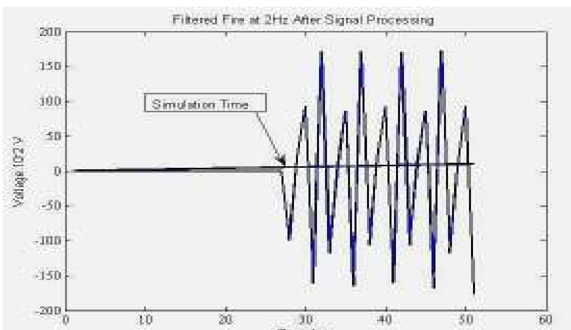

Figure 15. Radiation at 50Hz after DSP

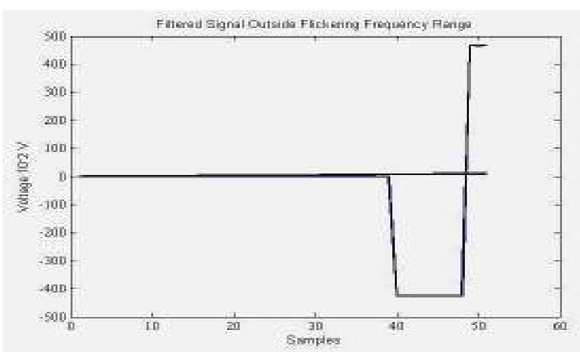

Figure 16. Fire Radiation after DSP

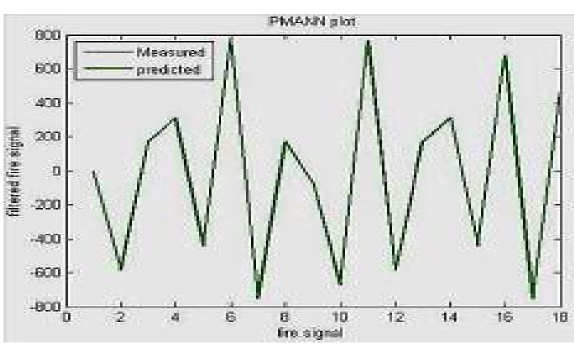

Figure 17. PMANN training of signal at 13Hz (ideal, hence the perfect match of both graphs)

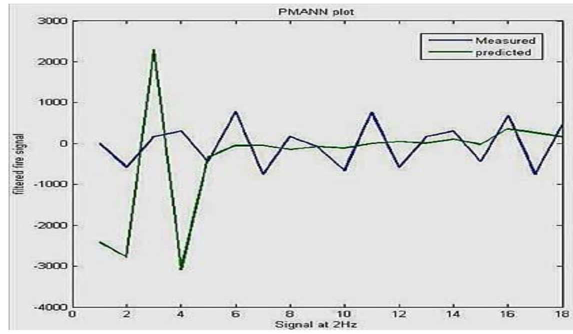

Figure 18. PMANN analysis of signal at 2Hz

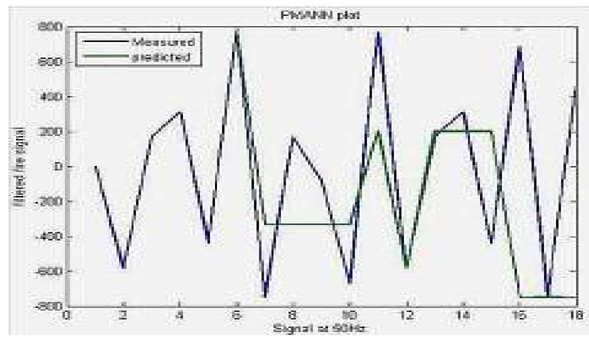

Figure 19. PMANN training of signal at 50Hz

Using the ICC, the samples (or coefficients) were analysed and decisions were made for "fire" and "non-fire" scenarios. Tables 2, 3 and 4 explain the decision rule. Our estimated reliability between the 13Hz sample signal and fire training signal gave 1, with 95% CI (1.00), which matches exactly. Hence, such a scenario is is recorded "fire" (see Table 2). As indicated in Table 3, our estimated reliability between the 2Hz sample signal and fire training signal gave an average of 0.004, with 95% CI (-1.660, 0.627), which is a miss-match. Hence, such a scenario is recorded "non-fire". Moreover, Table 4 shows that our estimated reliability between the 50Hz sample signal and fire training signal is an average of 0.144, with 95% CI (-1.222, 0.670), which is a miss-match. Hence, such a scenario is recorded "non-fire".

If the model is to be implemented in real life using appropriate electrical equipment, the detection mechanism will record only real FIRE cases, and send electric signals to the suppression valves. For the control of valves along suppression systems pipelines, the model hydraulic solenoid valve responded perfectly as expected in real life.

Figure 20 obtained was consistent with that obtained through experiments. Three cases of the PIDC are studied. The stepwise input simulated the digital nature of real life signals. The graphs perfectly correspond to a device connected to a PIDC under the Zeigler-Nichols' Process Reaction method of tuning, where the delay time

(L) is common for all the controllers and the time constant (T1, T2, T3) can be calculated from the slope of the graph for each PIDC. Hence, it will perfectly control depending on the nature of the pipeline to which it is connected to. From the graph, the 'PID' controller gives a normal forward control or open-loop control whereby the valves open and close. It is the most suitable PIDC for this application. Controllers 'PID1'and 'PID2', gave results for closed-looped control systems. Such systems experience some measure of damping (represented by the zigzag portion of the graphs). The damping is due to feedback and feed forward mechanisms as the PIDC tries to eliminate error. From the graph 'PID1' and 'PID2' have damping amplitudes (or ratios) within the range of 0.2-0.3, which are within the Zeigler-Nichols range of 0.21-4.0 (Roland, 2001).

Table 2. Intraclass Correlation Coefficient for 13Hz Sample Signals (e.g. open fires)

13Hz Sample Signal	Intraclass Correlation	95% Confidence Interval (CI)		F Test with True Value 0			
		Lower Bound	Upper Bound	Value	df1	df2	Sig
Single Measures	1.000	1.000	1.000	1.946E19	18	18	0.000
Average Measures	1.000	1.000	1.000	1.946E19	18	18	0.000

Table 3. Intraclass Correlation Coefficient for 2Hz Sample Signals (radiations from sources like Humans)

2Hz Sample Signal	Intraclass Correlation	95% Confidence Interval (CI)		F Test with True Value 0			
		Lower Bound	Upper Bound	Value	df1	df2	Sig
Single Measures	0.002	-0.454	0.457	1.004	17	17	0.497
Average Measures	0.004	-1.660	0.627	1.004	17	17	0.497

Table 4. Intraclass Correlation Coefficient for 50Hz Sample Signals (background radiations)

50Hz Sample Signal	Intraclass Correlation	95% Confidence Interval (CI)		F Test with True Value 0			
		Lower Bound	Upper Bound	Value	df1	df2	Sig
Single Measures	0.078	-.379	0.504	1.168	18	18	0.373
Average Measures	0.144	-1.222	0.670	1.168	18	18	0.373

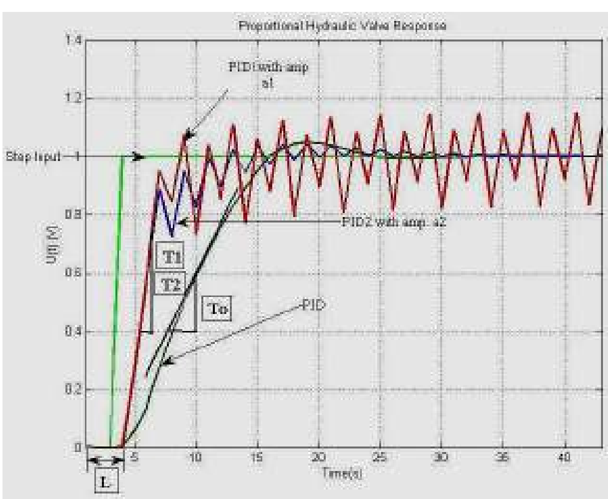

Figure 20. Hydraulic Proportional Valve Response.

5. Conclusion

An adaptive model for fire detection and suppression system has been discussed with emphasis on automatic fire detection and controlled suppression mechanism. First, the sensor was modeled using Laplace transforms and the fire signal detection mechanism was modeled using the Hamming window function and discrete wavelet transforms. Then using a PMANN and ICC as the decision rule, our detector could differentiate between fire and non-fire radiations. Using model equations of a PIDC and the standard dynamic equation for a proportional hydraulic solenoid valve, with valve constant being unity, the suppression mechanism was studied and simulated.

The results shows that under normal conditions the valve will control suppression systems (e.g. water sprinkler lines, foam injection lines and other similar fire suppression methods) and close pump lines in case of fire. We must note that sprinklers used in buildings are temperature activated. These are different from those used outside and in areas such as oil and gas storage sites. In Nigeria, most sprinklers used in loading gantries at oil and gas storage sites are perforated cone shape extensions of fire water lines. The detector controlled valves can be used to operate such sprinklers. Better approaches can still be used to devise more efficient models to mitigate the devastating effects of fire in petroleum storage sites.

References:

Chang, J.I., Cheng-Chung, L. (2006), "A study of storage tank accidents", Journal of Loss Prevention in the Process Industries Vol. 19 pp. 51–59.

Chukwuka, G.M., Aderemi, O.A., and Obolo, M.O., (2014), "Oil well characterization and artificial gas lift optimization using neural networks combined with genetic algorithm", *Discrete Dynamics in Nature and Society*, Vol.2014, DOI: http://dx.doi.org/10.1155/2014/289239

Emin B.S. (2009), *Pyro-electric Infrared (PIR) Sensor Based Event Detection*, Unpublished MSc Thesis, Department of Electrical and Electronics Engineering and the Institute of Engineering and Sciences, Bilkent University.

Fatih, E., Toreyin, B.U., Soyer, E.B., Inac, I, Gunay, O., Kose, K. and Cetin, E.A, (2012),"Wavelet based flickering flame detector using differential PIR sensors", *Fire Safety Journal*, Vol. 53, pp. 13-18.

Hamdan, Majed (Marv) and Gao, Zhuqiang (2007), *A Novel PID Controller for Pneumatic Proportional with Hysteresis*, Unpublished M.S. Thesis, Department of Electrical Engineering, Cleveland State University.

Javid, J.H., Shankar, B.B, Alan, W. and Zvi, B., (2008), "An adaptive method for hydrocarbon flame detection", *Neural Networks*, Vol. 21, pp. 398–405.

Lai, W.K., Rahmat, M.F., and Abdul Wahab, N., (2012), "Modeling and controller design of pneumatic actuator system with control valve", *International Journal on Smart Sensing and Intelligent Systems*, Vol. 5, No. 3, pp.624-644.

Li Z., Kaufman Y.J., Ichoku, C., Fraser, R., Trishchenko, A., Giglio, L., Jin, J. and Yu, X., (2000), *A Review of AVHRR-based Active Fire Detection Algorithms: Principles, Limitations, and Recommendations*, Canada Centre for Remote Sensing, Ottawa, Canada, and NASA Goddard Space Flight Center, Greenbelt, MD.

Munaf, F.B., (2008), "Position Control System of Hydraulic Cylinder Based on Microcontroller", Journal of Engineering and Development, Vol. 12, No. 3.

Nolan, D.P, (1996), *Handbook of Fire and Explosion Protection Engineering Principles for Oil, Gas, Chemical, and Related Facilities*, 1st edition, Noyes Publications, USA.

Odon, A. (2010), "Modeling and simulation of the pyro-electric detector using MATLAB/Simulink", *Measurement Science Review*, Vol.10, No. 6, pp.195-199.

Ogata, Katsuhiko (2010), *Modern Control Engineering*, 5th edition, Prentice Hall, Upper Saddle River, New Jersey, USA.

Persson, Henry and Lönnermark, Anders (2004), *Tank Fires: Review of Fire Incidents 1951–2003*, BRANDFORSK Project, SP Swedish National Testing and Research Institute, , Boras, Sweden.

Measurement Specialities, Inc, (1999), *Piezo Film Sensors Technical Manual* , Forge Avenue, Norristown, PA, USA.

Robert, J.S. and Sandra, L.H, (2012), *Fundamentals of Digital Signal Processing Using MATLAB*, 2 edition, Cengage Learning, First Stamford Place, Stamford, USA.

Roland, S.B., (2001), *Advanced Control Engineering*, 1st edition, Butterworth-Heinemann, Linacre House, Jordan Hill, Oxford, UK.

Schneiders, M.G.E., (2001), *Wavelets in Control Engineering*, Unblished Master's Thesis, Faculty of Mechanical Engineering, Dynamics and Control Technology, Eindhoven University of Technology.

Wikipedia (2015), *Automatic Fire Suppression*, Accessed 25th February 2015 from http://en.wikipedia.org/wiki/Automatic_fire_suppression

Yong, Z.Q. (2009), Control of Pneumatic Systems for Free Space and Interaction Tasks with System and Environmental Uncertainties, Unpublished PhD Thesis (Mechanical Engineering), Faculty of the Graduate School, Vanderbilt University

Authors' Biographical Notes:

Olawale Saheed Ismail *is a lecturer at the Department of Mechanical Engineering, University of Ibadan. He is presently on Sabbatical leave at the Department of Civil Engineering, University of Liberia, as a faculty contract staff with the USAID program.*

Chimsom. I. Chukwuemeka *graduated from the Department of Mechanical Engineering, University of Ibadan, Ibadan, Oyo State, Nigeria.*

■